Evaluation of Radiation Streaming Effects Due to Slit-Shaped Defects in HTGR Microreactor Transportation Casks

Woo Seok Choi, Jeong Ik Lee
∗ Dept. Nuclear & Quantum Eng., KAIST, 373-1, Guseong-dong, Yuseong-gu, Daejeon, 305-701, Republic of Korea
* Corresponding author: jeongiklee@kaist.ac.kr

***Keywords : Microreactor, Radiation Streaming, OpenMC**

1. Introduction

A mobile microreactor currently under development for defense and remote power supply requires rapid deployment and withdrawal. Unlike conventional nuclear power plants, where spent fuel requires years of cooling before transport, the mobile reactor must be recovered as a complete unit via truck or ship after a relatively short cooling period (within one year) following mission completion.

Particularly, the TRISO-based high-temperature gas-cooled reactor (HTGR) offers inherent safety advantages, but its high residual heat and source term at the time of transport pose significant challenges for transport container design. The U.S. PNNL report addresses transport accident scenarios for such micro-reactors, mentioning the possibility of fissures forming in the shielding due to impact or thermal stress, creating radiation streaming pathways [1]. Due to the short cooling period, minute shielding defects can cause severe localized exposure under high source conditions, but quantitative evaluation of the exposure under such circumstances is currently lacking.

Therefore, this study evaluates the sensitivity of radiation streaming when a fine slit-shaped defect is assumed in the shielding layer of a transport cask for a mobile TRISO-HTGR microreactor that has been cooled for one year after three years of operation. A fixed source term deprived from the PNNL report and a simplified surrogate geometry model were implemented in the OpenMC Monte Carlo code [2] to quantify how the external dose rate responds to slit width under 1-year cooling transport conditions.

2. Computational Model and Methods

The subject of analysis in this study is a 20 MWth mobile high-temperature gas reactor (HTGR) using HALEU UCO TRISO fuel. The source term is based on the inventory at the point of 1-year cooling, considering a rapid retrieval scenario after 3 effective power years (EFPY) of operation. This represents a conservative condition compared to the typical 5-year cooling period, for which the total radioactivity is higher and, in particular, the intensity of high-energy gamma rays and neutron sources, which are sensitive to shielding, remains elevated. The radionuclide inventory applied in this study was derived from the PNNL report, which incorporates X-energy's scoping inventory data. This selection focuses on 49 major nuclides with activities exceeding 0.1 Ci after a one-year cooling period. The radioactivity inventory for each major nuclide at the one-year cooling point applied in this study is shown in Table I.

Table I. Major Radionuclide Inventory for 1-year Cooled 20 MWt HTGR

Nuclide	Activity (Ci)	Activity (Bq)	Note
Ce-144	3.41E+5	1.26E+16	Major Source
Pr-144	3.40E+5	1.26E+16	High Energy Gamma
Cs-134	7.78E+4	2.88E+15	High Energy Gamma
Cs-137	9.03E+4	3.34E+15	Major Gamma Source
Ba-137m	8.55E+4	3.16E+15	Daughter of Cs-137
Cm-244	1.26E+3	4.66E+13	Major Neutron Source
Other	5.76E+5	2.13E+16	-
Total	1.51E+6	5.59E+16	99% of Total Inventory

For gamma sources, Ce-144, Cs-137, and their daughter nuclides provide the dominant contribution. For neutron sources, considering the characteristics of high burnup TRISO fuel, calculations account for spontaneous fission and (α, n) reactions of transuranic (TRU) nuclides, including Cm-244.

Table II. Source Term Distribution

Nuclide	Activity (Bq)	TRISO	Core	Pressure Boundary
Ce-144	1.26E+16	1.26E+16	4.13E+11	2.67E+9
Pr-144	1.26E+16	1.26E+16	4.11E+11	2.67E+9
Cs-134	2.88E+15	2.88E+15	4.17E+11	4.72E+11
Cs-137	3.34E+15	3.34E+15	4.84E+11	5.48E+11
Ba-137m	3.16E+15	3.15E+15	1.06E+13	5.98E+10
Cm-244	4.66E+13	4.66E+13	1.37E+9	7.09E+5
Other	2.13E+16	2.13E+16	1.08E+13	2.46E+11
Total	5.59E+16	5.59E+16	2.31E+13	1.33E+12

In radiation streaming analysis, not only the total source strength but also spatial distribution has a decisive influence. As shown in Table II, this study modeled source distribution into the following three regions according to the Material Hazard Rating (MAR) classification system from the report: (1) The TRISO-

retained region (Retained in TRISO) within the fuel particles, (2) the core material hold-up region (Core Material Hold-up) diffused during operation and deposited on structural materials like the graphite matrix, and (3) the pressure boundary plateout region (Pressure Boundary Plateout) deposited on the inner wall of the primary system pressure vessel. The plateout source, in particular, is considered the dominant source term with the highest potential for leakage to the outside without distance attenuation when shielding defects occur, as it is in direct contact with the inner surface of the shielding.

While the 1-year cooled radionuclide inventory and its spatial partitioning based on the MAR classification (Tables I and II) were directly adopted from the reference report, the three-dimensional transport geometry was independently postulated for this study. The homogenized core dimensions, multi-layer shielding configuration, and the through-thickness slit parameters were intentionally designed to establish a bounding, conservative model for maximizing radiation streaming. Consequently, the derived dose rate sensitivities reflect the behavior of this specific hypothetical configuration and should not be construed as a universal defect acceptance criterion.

3. Methodology

In this study, to evaluate the radiation streaming effects caused by shielding defects during the transport of a TRISO fueled microreactor, the reactor module and its transportation cask were modeled as three-dimensional geometries using OpenMC, as illustrated in Fig 1 and Fig 2.

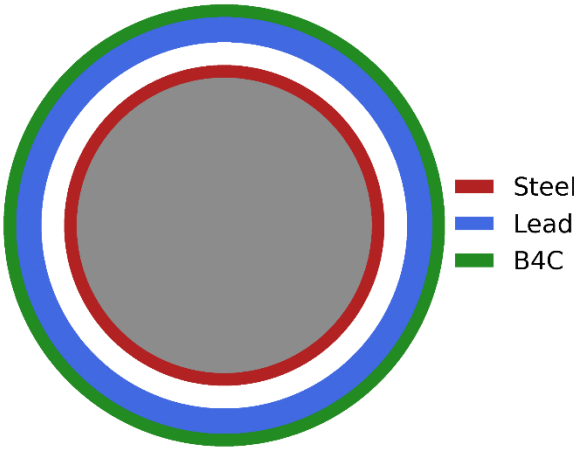

Fig 1. Simplified Geometry of HTGR Microreactor Cask

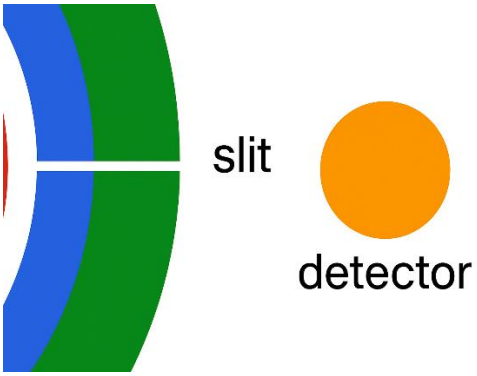

Fig 2. Defect Definition and External Detector Location

The 20 MWth prismatic HTGR core was modeled as a homogenized cylinder (radius 1.17 m, height 2.34 m) based on the HTR-10 reference power density of 2.00 MW/m³. These dimensions were selected to provide a representative surrogate core for transport dose calculations and are not directly adopted from PNNL report. Rather than explicitly modeling the heterogeneous microstructure of TRISO particles and graphite blocks, the core was treated as a homogenized volumetric source. This intentional simplification neglects the inherent self-shielding effects of the fuel kernels and graphite matrix, thereby establishing a strictly conservative bounding condition that maximizes the calculated external dose rates.

The shielding configuration of the transportation cask adopts a representative multi-layer concept for mobile reactors, designed to minimize radiation leakage. Drawing upon the pressure vessel specifications of the URENCO U-Battery (20 MWth) [3] and the shielding design of the KAIST MMR [4], the cask structure was modeled as concentric cylindrical layers enveloping the core. It comprises a 10 cm thick steel pressure vessel as the innermost boundary, followed by a 20 cm thick Lead monoxide (PbO) gamma shield, and a 10 cm thick boron carbide (B_4C) neutron shield as the outermost layer. These layer materials and thicknesses are representative assumptions for sensitivity analysis and are not intended to reproduce a specific cask design in PNNL

The hypothetical shielding defect was modeled as a vertical slit penetrating the entire thickness of both the PbO and B_4C layers. An axial height of 350 cm, extending 58 cm beyond both the top and bottom of the 234 cm active core, was selected. This substantial margin eliminates edge-shadowing effects in the model, ensuring a bounding line-of-sight condition from the active core volume to the detector. Accordingly, the defect geometry and height should be interpreted as a conservative sensitivity assumption rather than a prediction of an actual crack shape in an accident. Dose rates were evaluated at a location 1 m from the external surface of the cask, consistent with the measurement distance specified in 10 CFR 71.51 [5].

To obtain a receptor-scale estimate while maintaining tractable Monte Carlo uncertainty, the particle fluence was scored in an air-filled spherical scoring region (radius 15 cm) centered at the receptor location. This radius matches the ICRU sphere (30 cm diameter) [6], a widely used reference phantom size for defining operational dose quantities in external radiation fields, and the resulting fluence is interpreted as a spatially averaged field at the receptor position. Effective dose was then estimated using fluence-to-effective dose conversion coefficients for AP geometry from ICRP Publication 116 [7], as provided by the OpenMC dose coefficients implementation. All dose rates reported in this paper correspond to ICRP-116 fluence-to-effective dose estimates in AP geometry and are used as an operational proxy for discussing the 1-m criterion in 10 CFR 71.51, rather than a definitive licensing quantity. To reduce Monte Carlo variance for rare streaming trajectories, weight windows were trained on the most challenging narrow-slit case using a fixed regular mesh/energy structure and then applied unchanged to all slit widths.

4. Result and Discussion

Table III summarizes the calculated dose rates for six slit scenarios (width = 0, 0.1, 0.2, 0.4, 1.0, and 2.0 cm). The total dose rate is dominated by the photon contribution, particularly as the slit width increases.

Table III. Calculated Photon and Neutron Dose Rates by Slit Width

Slit width (cm)	Photon dose (μSv/h)	Neutron dose (μSv/h)	Total dose (μSv/h)	Total relative error
0.0	1.89E-02	1.35E-02	3.24E-02	20.1%
0.1	6.89E-02	9.58E-03	7.84E-02	12.1%
0.2	3.29E-01	9.60E-03	3.39E-01	9.5%
0.4	1.25E+00	9.62E-03	1.26E+00	6.8%
1.0	2.50E+01	1.52E-02	2.50E+01	6.3%
2.0	8.98E+01	2.02E-02	8.98E+01	5.8%

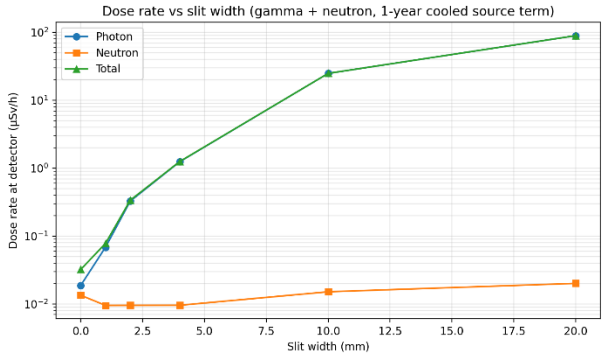

Fig 4. Comparison of Dose Rate by Slit Width

As shown in Fig. 4, the photon dose rate increases monotonically from 1.89×10^{-2} μSv/h for the intact case (0.0 cm) to 8.98×10 μSv/h for the 2.0 cm slit case. This phenomenon indicates that high-energy photons can stream efficiently through small gaps, increasing the total dose by more than three orders of magnitude. In contrast, the neutron dose remains nearly constant at the order of 10^{-2} μSv/h for all cases because the remaining shield still provides substantial attenuation.

When compared to the 10 CFR 71.51(a)(2) limit for Hypothetical Accident Conditions (10 mSv/h at 1 m), all discrete cases analyzed here remain well below the regulatory threshold. Because only a limited set of slit widths and a simplified geometry were considered, and because the dose response depends strongly on the source distribution, shielding design, and defect geometry, it is not appropriate to infer a universal critical slit width from interpolation. Instead, the present results suggest that sub-centimeter defects can materially change external dose rates under early-transport source terms, highlighting the need for design-specific defect tolerance evaluation.

5. Conclusions

In this study, the impact of shielding defects on radiation streaming was quantitatively evaluated for a HTGR microreactor transport cask under a 1-year cooling scenario. A simplified OpenMC fixed-source model was utilized to simulate direct radiation streaming through slit-shaped defects in a multi-layer shielding configuration. The radionuclide inventory and the MAR-based source partitioning were referenced from the reference report, while the transport cask geometry and defect definitions were provided as conservative modeling assumptions to perform a sensitivity assessment of streaming behavior.

The results demonstrate that the detector dose rate increases monotonically with slit width, exhibiting an increase of more than three orders of magnitude when the total dose expands from 3.24×10^{-2} μSv/h for the intact case to 8.98×10 μSv/h for the 2.0 cm slit case. The total dose is overwhelmingly driven by photon streaming, while the neutron contribution remains at the order of 10^{-2} μSv/h and becomes negligible relative to photons as the slit widens. This highlights that even millimeter-scale defects in the gamma shield can significantly degrade radiation safety margins for early-transport scenarios, depending on the specific design and source term.

Although the variance reduction technique using weight windows enabled stable evaluation, narrow-slit configurations still presented statistical challenges due to the rarity of streaming events. Future work will extend this analysis to include explicit heterogeneous core modeling to account for self-shielding effects, additional defect geometries, such as finite-length slits and tortuous cracks, and comparative studies with deterministic transport methods to better quantify uncertainties.

ACKNOWLEDGEMENTS

This work was supported by the National Research Foundation of Korea (NRF) grant funded by the Korea government (MSIT) (RS-2023-00259713).

REFERENCES

[1] G. A. Coles et al., “Parametric Study of Factors that Affect Calculated Dose from TRISO Fueled Microreactor Transportation Accident,” PNNL-33607, Pacific Northwest National Laboratory, Richland, WA (2022).
[2] P. K. Romano and B. Forget, “The OpenMC Monte Carlo particle transport code,” Ann. Nucl. Energy, 51, 274-281 (2013).
[3] Ding, M., Kloosterman, J. L., Kooijman, T., Linssen, R., Abram, T., Marsden, B., & Wickham, T. (2011). *Design of a U-Battery*® (Report No. PNR-131-2011-014). Delft University of Technology.
[4] Yu, H., Hartanto, D., Moon, J., & Kim, Y. (2015). A conceptual study of a supercritical CO2-cooled micro modular reactor. *Energies*, *8*(12), 13938-13952.
[5] Packaging and Transportation of Radioactive Material, 10 C.F.R. § 71 (2026).
[6] International Commission on Radiation Units and Measurements, "Determination of Dose Equivalents Resulting from External Radiation Sources," ICRU Report 39, Bethesda, MD (1985)
[7] ICRP, "Conversion Coefficients for Radiological Protection Quantities for External Radiation Exposures," ICRP Publication 116, Ann. ICRP, 40(2-5) (2010).